Proceedings of the
Annual Stability Conference
Structural Stability Research Council
San Antonio, Texas, March 19-22, 2024

Experimental testing of single-overhanging I-shaped steel girders

Maha Essa[1], Robert G. Driver[2], Ali Imanpour[3]

Abstract

Cantilever–suspended-span construction, commonly referred to as Gerber girder systems, is a common roof-framing system for single or multi-story buildings in North America. This system offers several advantages, such as ease of erection, reduced moments and lower deflections in comparison to simply-supported girders, due to the continuity of the cantilever segment over the column support. Nevertheless, it has become clear due to several collapses in Canada and the United States that the stability response of these systems is complex and in need of further investigation. Moreover, there are no special design guidelines in the Canadian and American steel design standards, despite the wide use of Gerber systems in practice, leading to disparate methods used by designers. This paper presents full-scale experimental testing of single-overhanging steel girders performed to investigate the stability response of steel Gerber systems. The test matrix explores various lateral bracing conditions expected in practice, including top-flange-only bracing, top and bottom flange bracing, and an unbraced cantilever tip, as well as various loading conditions to reproduce patterned gravity plus wind loading scenarios. The experimental results show that the addition of top flange lateral restraint at the cantilever tip is more effective at increasing the capacity of the overhanging girder than adding a bottom flange brace at the back span load location closest to the interior support. Furthermore, the method proposed by the Canadian Institute of Steel Construction underestimates the flexural capacity of the overhanging girders tested here.

1. Introduction

The Gerber system, also known as cantilever-suspended-span construction, is a commonly used method for framing roofs in light single-storey buildings in North America. As depicted in Fig. 1, this method involves a series of simply-supported girders that extend beyond the column as cantilevers, and the portion of the girder between the supports is called the back span. Drop-in spans, also known as suspended spans, are connected at the cantilever ends through a shear connection in alternate bays, and open-web steel joists (OWSJs) are frequently used as secondary framing members.

Due to the continuity between adjacent bays, negative moments (where the top flange is in tension) are introduced at the supports. Consequently, the girder needs to resist lower magnitudes of

[1] M.Sc. Student, University of Alberta, essa@ualberta.ca
[2] Professor, University of Alberta, rdriver@ualberta.ca
[3] Associate Professor, University of Alberta, imanpour@ualberta.ca

positive moments (where the bottom flange is in tension), as shown in Fig. 2. This balanced moment distribution in Gerber girders allows for a more efficient design, since lighter and shallower girders are sufficient to carry the same loads compared to simply-supported spans that lack continuity over the vertical support. Moreover, the deflection limits are easily satisfied by taking advantage of the continuity of the overhanging girders. Finally, the Gerber system avoids the need for costly and complex moment connections, making the construction process faster and resulting in lower deflections compared to conventional roof girders (Rongoe 1996).

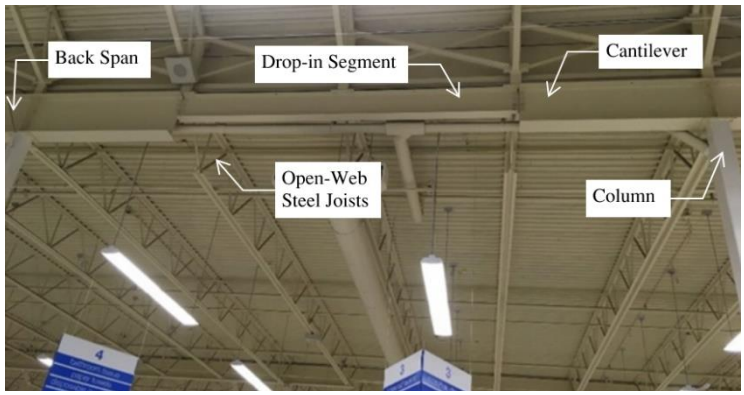

Figure 1: Gerber system in roof framing of a single-story retail building.

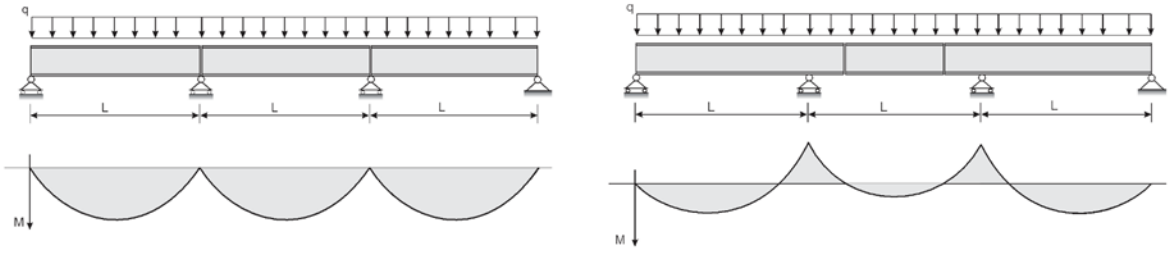

a) Bending Moment Diagram (Conventional Roof Girders) b) Bending Moment Diagram (Gerber Roof Girders)

Figure 2: Bending moment diagrams for roofing system with simply-supported girders and Gerber roof girders.

Despite the widespread use and benefits of the Gerber system in steel buildings across North America, little guidance on the design of these systems is provided by current steel design standards in both Canada, the Canadian steel design standard, CSA S16 (CSA 2019) and the United States, AISC Specification for Structural Steel Buildings, AISC 360-22 (AISC 2022). Several collapses, such as the roof collapse in a Burnaby, BC supermarket in 1988 (Closkey 1988) and a warehouse collapse in Texas in 2011, as well as more recent collapses in Halifax in 2015 and Montreal in 2019 (Metten 2019) highlight the need to reassess the stability response of these systems—especially their susceptibility to lateral-torsional buckling (LTB) and the need for proper bracing strategies, e.g., at the column locations.

A method for determining the elastic buckling resistance of an overhanging girder, which consists of a back span and a cantilever segment, was proposed by Essa and Kennedy (1993). The method is based on interaction buckling, which accounts for the beneficial restraint provided by the less critically loaded segment on the more critically loaded segment in an overhanging beam. The

interaction method requires first treating the back span and cantilever segments separately, calculating a critical elastic moment for each segment. The proposed method for determining the critical elastic moment of the cantilever accounts for either a top flange or shear centre load applied at the cantilever tip, and assumes the back span is unrestrained and unloaded between vertical supports, where lateral deflections and cross-sectional twist are prevented, while allowing the section to warp.

The Canadian Institute of Steel Construction (CISC) (1989) presented a design procedure for Gerber roof framing applications based on the recommendations of the SSRC Guide (Galambos 1988) on the design of overhanging beams which considers the back span separately from the cantilever segment. The critical elastic moment of the back span is calculated using the Roeder and Assadi (1982) equation for beams with continuous tension flange bracing along the entire length, and the resistance of the cantilever portion of the overhanging beam is checked by accounting for lateral restraint and load height provided to the tip of the cantilever, and the effect of the continuity of the cantilever segment over the column, using the effective length concept introduced by Kirby and Nethercot (1979). A more recent publication from CISC, Design Module 8 on Single-Storey Building Design (Lasby 2019), also requires treating the cantilever and back span segments separately. Two checks are done for the back span: one for the maximum positive moment and one for the maximum negative moment. The check for the maximum positive moment on the back span calculates the critical elastic moment using the unbraced segment between lateral restraints on the back span subjected to the most critical bending moment gradient (i.e., closest to uniform bending). The critical elastic moment for the back span under maximum negative moment is calculated assuming the entire length of the back span as the unbraced length, obtaining a moment gradient factor considering loading along the entire back span. Lastly, the cantilever is checked under negative bending moment using the Essa and Kennedy (1994) interaction method, which assumes the entire length of the back span is unbraced. While Essa and Kennedy (1994) provide a moment gradient factor for calculating the critical elastic moment of the back span for use in the interaction equation, CISC (Lasby 2019) uses a conservative approach of assuming the back span is under uniform bending moment.

To check the cantilever segment of the overhanging girder, Nethercot (1973) proposed an effective length concept which assumes a cantilever span and a back span of equal length which is unloaded and unrestrained between supports; it was later found that the cantilever span should not be taken as less than the length of the back span (Kirby and Nethercot 1979). The effective length factors account for the type of loading, level of load application, and type of restraint at the tip of the cantilever. Trahair (1983) proposed an interaction method to calculate the elastic LTB capacity of a double-overhanging girder, using the buckling loads of the back span and cantilever segments separately, assuming the back span is free to warp at the supports while the cantilever is built-in (i.e., warping is prevented). The only loading scenario considered in the study was a concentrated load at the tip of the cantilever, applied either at the shear centre or top flange level.

Yura and Helwig (2010) performed various finite element simulations to propose several LTB modification factors for beams with reverse curvature bending, with either one or two inflection points along the span. Two cases were investigated: unbraced beams, where no intermediate bracing was provided along the length of the beam and loading was applied at the centroid of an I-shape, and gravity-loaded beams braced continuously on the top flange with load applied at the top flange.

While the experimental full-scale test database on the LTB response of simply-supported girders is plentiful, there remains a relatively small amount of such experimental data on the stability response of steel overhanging girders. Essa and Kennedy (1993) performed 33 full-scale tests on single-overhanging girders with a 7.31 long back span and 1.22 m long cantilever segment. The back span was tested under either five equally-spaced concentrated loads, one load at the midspan, or no loads; the cantilever was tested under one concentrated load at the tip. Factors such as load height, stiffeners at the supports, and lateral and torsional restraints at the load points were investigated. It was found that the effect of web distortion on the capacity of the girders became more significant as the load was applied higher above the shear centre, as well as in girders braced torsionally along one flange. The results of this test program confirmed that stiffeners can effectively eliminate web distortion, and bottom flange restraint provided at the fulcrum support help significantly increase the buckling capacity of the girder.

The evaluation of the stability response of overhanging girders used in Gerber system involves considering various factors, including loading and bracing conditions. Given the complex loading and bracing scenarios anticipated in Gerber roofing system, full-scale physical testing of overhanging girders exposed to different bracing and loading conditions is crucial for developing a practical design approach for overhanging girders. The goal of this research is to supplement existing knowledge about the capacity and behavior of steel cantilevered girders under different loading and restraint conditions at the cantilever tip and along the back span. The full-scale physical testing program composed of 14 single-overhanging girders is first presented, with the test specimen matrix based largely on numerical simulations, which highlighted the parameters most influential on the stability of overhanging girders. The experimental setup designed to perform these tests is then described, followed by analysis of the experimental results and comparison of the results with an existing design method. This effort aims to improve the understanding of the system's stability response and contribute to the development of a practical and efficient design method for these systems.

2. Test Specimen Matrix

As part of the broader research initiative, a numerical model (Esmaeili et al., 2021) has been developed for overhanging I-shaped steel girders. This model was used to identify key factors affecting the LTB capacity of such girders and played a role in designing the test specimen matrix. The main goal when developing this matrix was to select specimens and configurations covering various factors, such as loading and restraint conditions, to examine their impact on the stability of overhanging girders. Additionally, the effort aimed to build upon the existing overhanging girder test database provided by Essa and Kennedy (1993).

A typical single-overhanging I-shaped girder considered in the numerical study is shown in Fig. 3a, and Fig. 3b shows its bending moment distribution. In this figure, P_b refers to the point loads on the back span coming from secondary members such as open-web steel joists, P_{max} and P_{min} are the larger and smaller point loads at the cantilever tips, respectively, L_b represents the length of the back span, L_c is the length of the cantilever, s is the joist spacing, n equals the number of point loads on the back span plus 1, M^L_{max} is the local maximum bending moment along the back span, M_{Fmax} represents the bending moment at the fulcrum support, and κ_1' is defined as the ratio of M^L_{max} to M_{Fmax}.

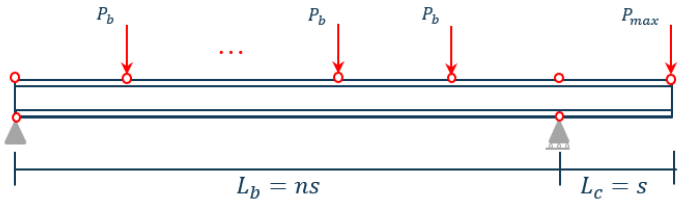

a) Single overhanging girder configuration.

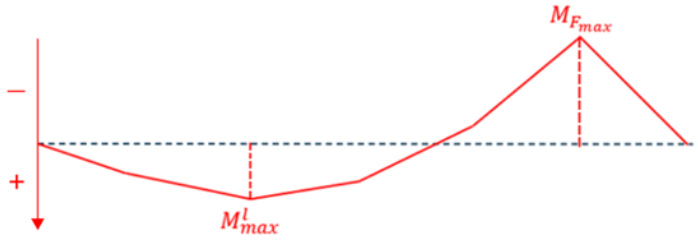

b) Bending moment diagram for single overhanging girder.

Figure 3: Typical single overhanging girder (symbol ○ represents point of lateral support).

While it is acknowledged in practice that connecting an OWSJ to the top flange of a Gerber girder provides both lateral and torsional restraint to the flange, the positive effect of torsional restraint was neglected in the test program. In a typical Gerber system, the cantilever tip faces two potential sources of loading: the first involves the load from the drop-in segment, transferred through a shear connection, and the second arises from the presence of an OWSJ framing into the top flange of the girder at the cantilever tip. If there is no OWSJ framing at this location, the cantilever tip is deemed unbraced, and the load applied at the cantilever tip originates solely from the shear connection with the drop-in segment, usually applied at or near the shear centre. For ease of implementation in the laboratory, however, all loads are applied at the top flange level in the experimental study, which is expected to create a more critical loading condition compared to shear centre loading due to the destabilizing effect of top flange loading. The test matrix incorporates the lateral bracing condition at the cantilever tip of an overhanging girder and the presence of a bottom chord extension on secondary members off the column line. This inclusion is achieved by categorizing the test specimens into five distinct groups based on their loading and restraint conditions (LRCs) as shown in Fig. 4. The naming scheme of the groups is as follows:

- LRC 1: C(U)–B(T): cantilever tip is unbraced and back span is laterally restrained at the top flange;
- LRC 2: C(T)–B(T): cantilever tip is laterally restrained at the top flange and back span is laterally restrained at the top flange;
- LRC 3: C(TB)–B(T): cantilever tip is laterally restrained at both the top and bottom flanges and back span is laterally restrained at the top flange;
- LRC 4: C(U)–B(TB): cantilever tip is unbraced and back span is laterally restrained at the top flange at all load locations, with an additional lateral restraint provided to the bottom flange at the first load point from the fulcrum (interior) support; and
- LRC 5: C(TB)–B(TB): cantilever tip is laterally restrained at both the top and bottom flanges and back span is laterally restrained at the top flange at all load locations, with an additional

lateral restraint provided to the bottom flange at the first load point from the fulcrum (interior) support.

In this experimental study, all test girders were 11.43 m long, spanning 10.97 m between the centerline of the support and the centerline of the load applied at the cantilever tip. An additional length of 0.228 m was provided on either end of the girder for configuration in the test frame. The loading of the test specimens includes four point loads at 1.83 m intervals along the 9.14 m long back span, denoted as P_b, and a point load applied at the tip of the 1.83 m long cantilever, referred to as P_{max}, as shown in Fig. 3a. In each of the LRCs, a unique load of P_{max} is applied at the cantilever tip. The load on the back span, P_b, is then adjusted as a fraction of P_{max} until a desired bending moment gradient is attained. This is quantified by the ratio κ_1''', representing the ratio of P_b to P_{max}, and can assume three values in the test matrix: 0.80, 0.38, or 0.25. A κ_1''' value of 0.80 corresponds to a κ_1' value of -2.00, κ_1''' equal to 0.38 corresponds to κ_1' equal to -0.73, and κ_1''' equal to 0.25 corresponds to κ_1' equal to -0.35.

The experimental study comprises 14 single-overhanging W410×85 test girders made of ASTM A992 steel with a specified yield stress of 345 MPa, as seen in Fig. 4. The cross-section conforms with the CSA S16-19 (CSA 2019) Class 1 flanges and web limits, where a Class 1 flange and web has a $b/2t$ less than or equal to 145 divided by the square root of the yield strength and $(d\text{-}2t)/w$ less than or equal to 1100 divided by the square root of the yield strength, respectively, where d is the section depth, b is the flange width, t is the flange thickness, w is the web thickness. In this paper, each test girder is denoted by an alphanumeric specimen identification (ID), reflecting the loading and restraint condition (LRC) as well as the load ratio, κ_1''', which is defined as the ratio of the load applied on the back span to the load on the cantilever tip. The naming convention follows 'LRC' (for loading and restraint condition), followed by the LRC number as reported previously, and, κ_1'''.

The test girders are each equipped with two full-depth web stiffeners, positioned at each support. While the unstiffened web crippling and yielding capacities at the support locations surpassed the maximum expected reactions in the tests, it is considered prudent to include web stiffeners at column locations for enhanced resistance to local instabilities (CISC 1989).

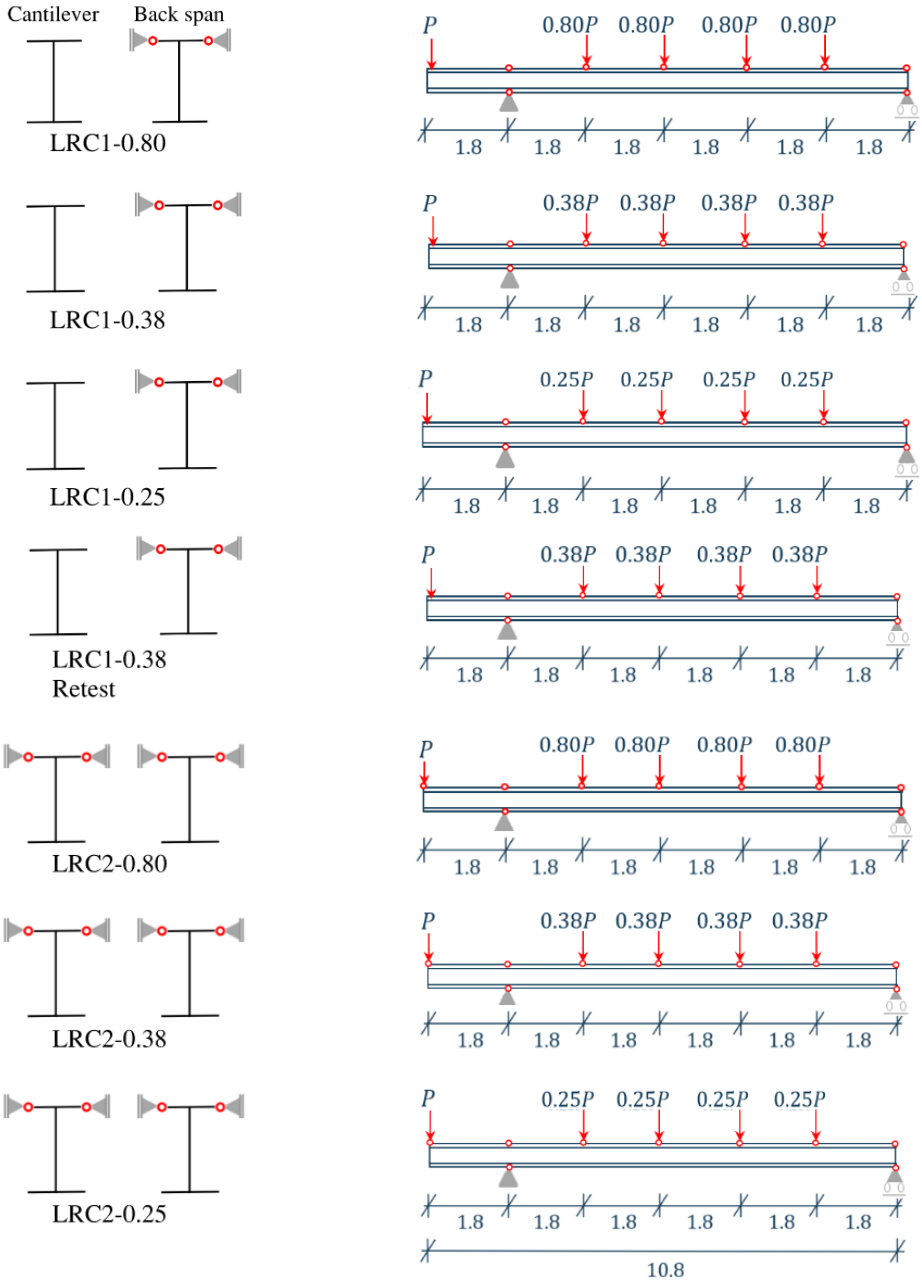

a) Test specimens: LRCs 1 and 2

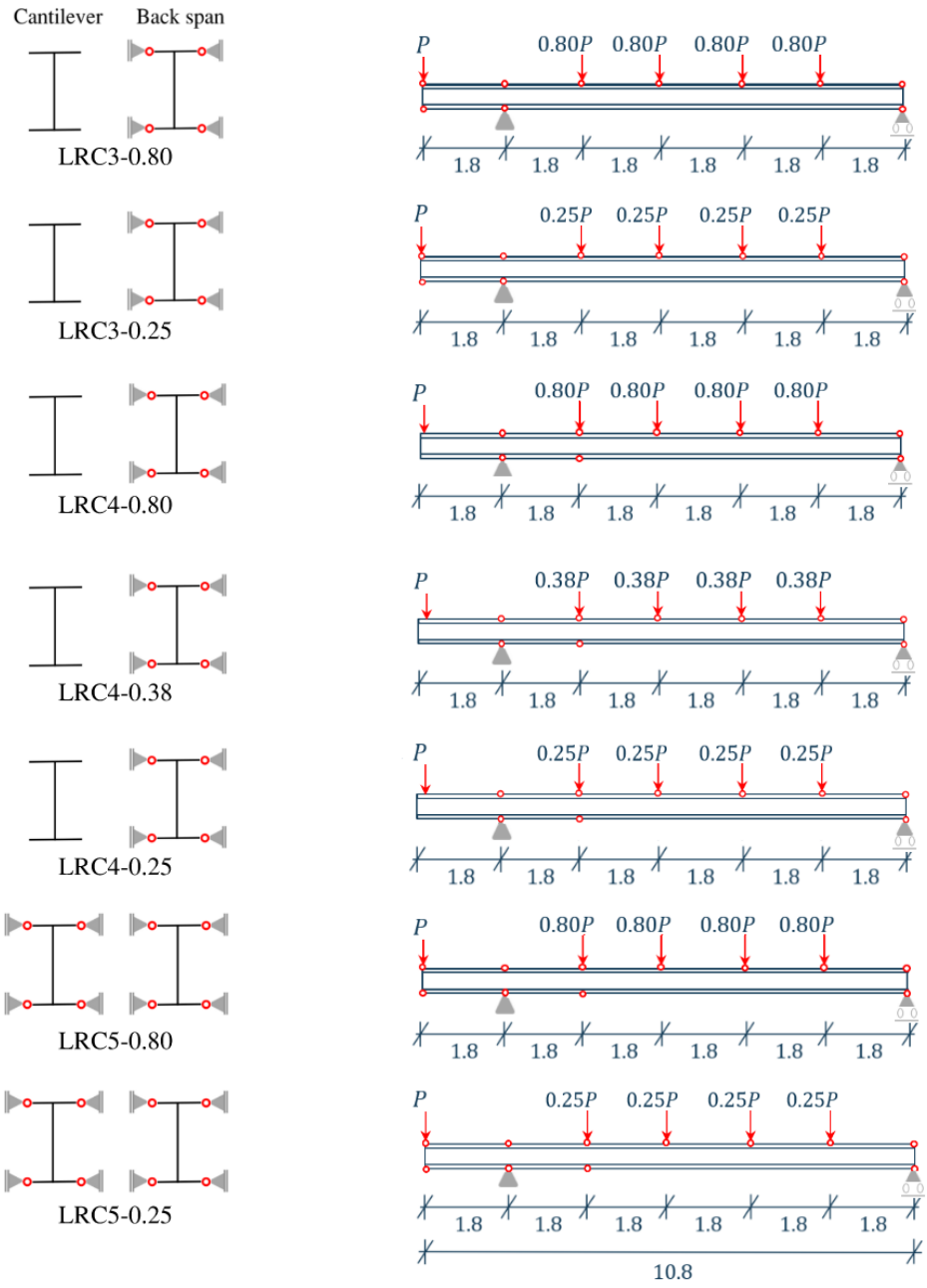

b) Test specimens: LRCs 3 - 5

Figure 4: Loading and restraint conditions of test specimens.

3. Test Setup

The test setup was designed to accommodate the expected girder displacements and rotations based on finite element (FE) simulations by Esmaeili et al. (2021), and drew largely from the Structural Stability Research Council (SSRC) Technical Memorandum No. 9 on flexural testing (Ziemian 2010). Fig. 5a displays a three-dimensional model of the test setup for the C(U)–B(TB) group (LRC 4), with the test specimen in blue and the load frame, bracing system, and supports in grey. The plan view in Fig. 5b, which outlines the directions referenced in the subsequent sections of this paper, provides an additional perspective on the test setup.

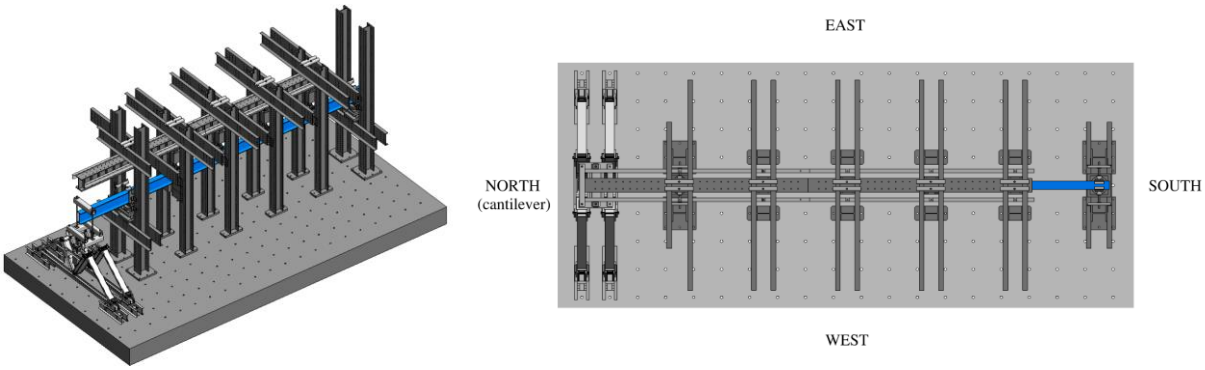

a) Three-dimensional model of experimental test setup

b) Cardinal directions on plan view of test setup

Figure 5: Experimental test setup

3.1 Gravity Load Application

As the cantilever tip can be either laterally braced or unbraced, two gravity load mechanisms are employed in the tests. In the first mechanism, utilized at load points where the girder is restrained from lateral movement (depicted in Fig. 6a), a hydraulic actuator applies the gravity load, generating a concentrated load on the test specimen. At the top end, the hydraulic actuators are pin-connected to a rigid reaction frame that transfers the reaction load to the laboratory strong floor through high-strength steel anchor rods. The reaction frame consists of a distributing beam connected to MC460×86 channels through a pair of hollow structural section HSS89×89×9.5 and ASTM A354 Grade B4 threaded rods, spanning across two columns on either side of the girder. All components of the reaction frame were analyzed under the maximum expected loads obtained from FE simulations to ensure yielding of the fixtures does not occur during a test. At the bottom end, the actuator is pin-connected to a semi-cylindrical bearing with its axis aligned with the longitudinal axis of the test specimen. This bearing rests on the top flange of the girder, allowing for cross-section twist while maintaining a stable mechanism with the pin-ended hydraulic actuator.

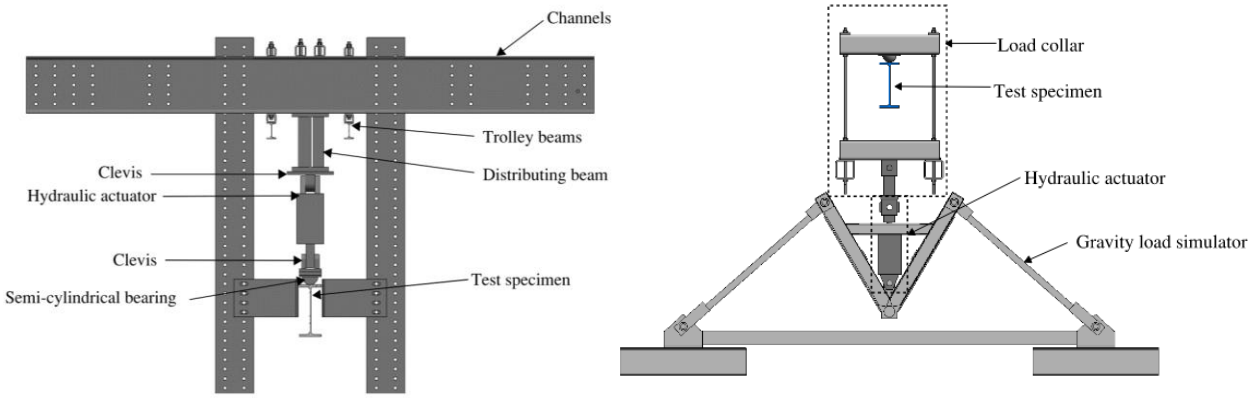

a) Gravity load mechanism at laterally braced load points b) Gravity load mechanism at unbraced cantilever tip.

Figure 6: Gravity load mechanisms

The second gravity load mechanism, used when the cantilever tip is laterally unbraced, comprises three pivot pin-connected components: (1) gravity load simulator (GLS)—a pin-jointed mechanism designed for testing structures experiencing sidesway under a load (Yarimci et al., 1967), (2) hydraulic actuator, and (3) load collar, as depicted in Fig. 6b. The GLS can freely displace up to 400 mm from its equilibrium position in either direction while maintaining a nearly vertical point load. It has an in-plane load capacity of 360 kN (Driver et al., 1997). Since the maximum load expected in the tests is 394 kN, exceeding the capacity of a single GLS, two GLSs are utilized at the cantilever tip, connected using HSS sections. At the start of a test, the hydraulic actuator is extended by 76 mm, allowing for either upward or downward vertical deflection. As it retracts, the hydraulic actuator pulls on the load collar, delivering a downward concentrated force to the top flange of the test girder. The load collar accommodates cross-section twist by featuring a hemispherical bearing on the top flange. The design choice of a hemispherical bearing as part of the load collar assembly, as opposed to a semi-cylindrical bearing, allows the girder to undergo in-plane bending without relying on pin-ended hydraulic actuators.

3.2 Boundary Conditions

The experimental test setup simulates column locations in a typical Gerber frame at the supports. Similar configurations are applied to the support fixtures at both ends of the back span, resulting in a simply supported girder. In this setup, the specimen is free to displace longitudinally and is not restrained from warping. However, it is restricted from twisting and displacing laterally or vertically. This support condition is achieved by placing the specimen on a set of rollers, a load cell, and a knife edge, as illustrated in Fig. 7a. The rollers allow the girder to experience longitudinal displacement, with a maximum of 65 mm in either direction. To ensure stability, permitting loading to progress beyond buckling and into the post-buckling stage, only the roller at the south end remained unlocked (allowing longitudinal displacement) throughout the tests. Conversely, the roller at the north end, situated closest to the cantilever, is locked, effectively acting as a pin and allowing no more than 5 mm of longitudinal displacement. The knife edge facilitates in-plane pivoting of the girder, and the load cell is employed to measure the reaction forces at the supports.

To permit warping of the girder while simultaneously preventing twisting at the supports, four lateral braces are introduced at each support. Comprising Grade 5 (ASTM A449) fully-threaded rods, these braces are fitted with rollers at their ends, as depicted in Fig. 7a. Two of these braces—one at the top flange level and one at the bottom flange level—make contact with a steel plate on either side of the test specimen, providing a larger bearing area. This arrangement effectively restrains cross-section twist and lateral movement of the girder, while the rollers allow the girder to undergo warping and longitudinal displacement. Fig. 7b shows the bracing configuration at a load point on the back span.

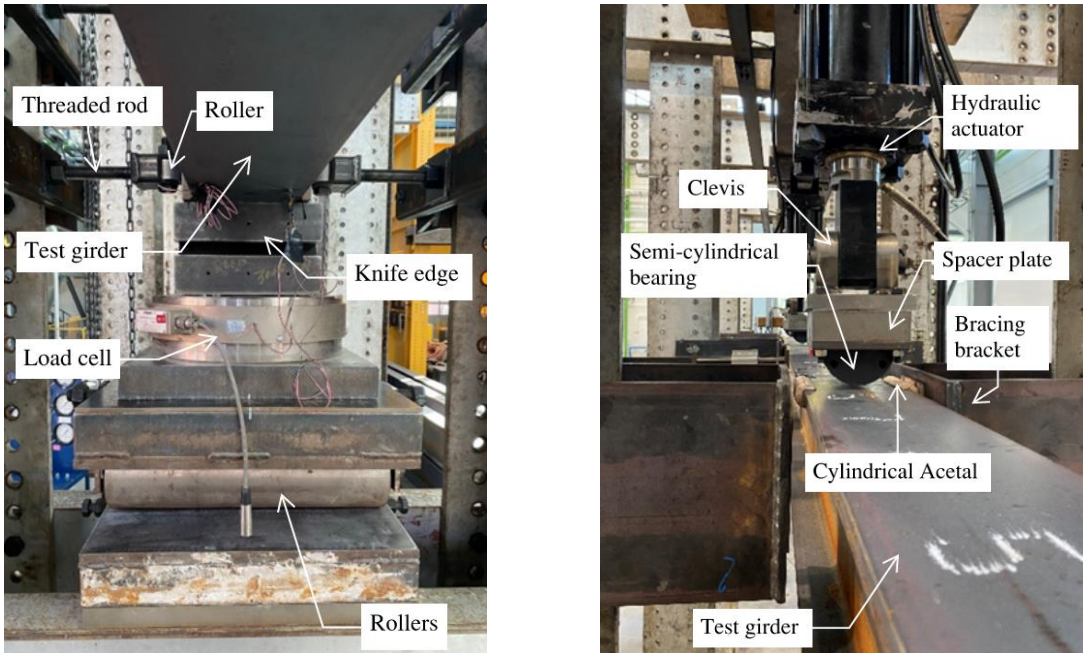

a) Vertical support in the longitudinal direction b) Bracing detail at back span loading points

Figure 7: Vertical support and load point details

3.3 Lateral Bracing

Lateral bracing is employed in the flexural testing of girders to prevent out-of-plane movement, simulating the restraint provided by OWSJs in a typical Gerber frame. Given that the test girder is expected to deflect vertically along the back span and cantilever, it is crucial to utilize a lateral bracing mechanism that allows for unrestricted vertical movement while simultaneously restricting movement perpendicular to the girder web to avoid unintended restraint.

The solution involved using a U-shaped bracing bracket, depicted in Fig. 7b, bolted to the Meccano columns on either side of the girder where lateral bracing is necessary. These brackets are equipped with an Acetal sheet attached to the front plate. Acetal is a composite of Teflon™, with a very low coefficient of friction, and Delrin®, providing hardness to prevent significant deformation under load. To further reduce friction between the sliding surfaces, a cylindrical Acetal bearing is placed on the flange of the girder, resulting in Acetal-on-Acetal interaction at the lateral bracing points. Both pieces of Acetal are coated with grease, ensuring minimal frictional forces as the girder deflects vertically while being restrained at the top flange from horizontal movement.

When only the top flange is to be braced as seen in Fig. 4 (LRC 2), only one of the U-shaped brackets is bolted to the columns on either side of the test girder to bear against the top flange. When both the top and bottom flanges are braced as seen in Fig. 4 (LRCs 3, 4 and 5), three of these U-shaped brackets are bolted underneath one another on the Meccano columns on either side of the girder, resulting in a total length of 915 mm. This accommodates the full depth of the girder in the undeflected position of 417 mm, as well as an extra 498 mm of space for the girder to deflect vertically while keeping both the top and bottom flanges bearing against the front Acetal sheet.

3.4 Initial Geometric Imperfections

Cross-section imperfections and global geometric imperfections were measured at seven equally spaced points, which corresponded with the points of load application and reactions. Table 1 summarizes the mean dimensions at the seven stations for each of the test specimens, where k is the distance between the extreme surface of the flange and the end of the fillet radius and k_2 is the distance between the edge of the web and the end of the radius. As the girders come from three different heats of steel, the measured yield stress of the flanges ($F_{y,f}$) and web ($F_{y,w}$) for each specimen is also given in Table 1.

Table 1: Measured cross-sectional dimensions of test specimens.

Specimen ID	d (mm)	b (mm)	t (mm)	w (mm)	k (mm)	k_2 (mm)	$F_{y,f}$ (MPa)	$F_{y,w}$ (MPa)
LRC1-0.80	417	182	18.2	11.6	38.8	21.3	345	373
LRC1-0.38	417	182	17.9	11.5	38.3	22.1	339	361
LRC1-0.38 Retest	418	182	18.0	11.7	38.6	23.7	332	353
LRC1-0.25	418	182	18.0	11.6	36.2	21.3	332	353
LRC2-0.80	416	182	17.8	11.5	39.8	20.6	345	373
LRC2-0.38	418	182	17.9	11.6	41.0	21.8	345	373
LRC2-0.25	419	181	18.0	11.8	38.7	21.7	345	373
LRC3-0.80	419	181	17.9	11.5	37.1	19.9	345	373
LRC3-0.25	418	181	17.8	11.7	33.8	20.8	345	373
LRC4-0.80	419	183	18.0	11.7	39.2	20.4	332	353
LRC4-0.38	417	182	18.2	11.5	36.8	21.1	339	361
LRC4-0.25	417	182	18.0	11.6	35.4	22.5	339	361
LRC5-0.80	419	182	18.0	11.7	41.2	21.2	345	373
LRC5-0.25	418	183	17.9	11.6	37.8	20.8	345	373

Measurements for initial geometric out-of-straightness such as sweep (lateral out-of-straightness), camber, and twist were taken at the seven stations along the girder with the girder on level pedestals on the strong floor. Sweep and camber were measured at the top and bottom flanges, while twist was measured at the web. Table 2 summarizes the initial geometric imperfections measured for all test specimens, reported as the maximum value measured among the seven stations. A positive sweep is taken as bowing towards the west side of the laboratory (see Fig. 5b), negative camber corresponds to a sag, and a positive twist value refers to clockwise rotation when looking at the girder from the south end (see Fig. 5b). In this table, L is the distance between the center of the end support assembly and the center of the bearing at the cantilever tip.

Table 2: Maximum initial geometric imperfections of test specimens

Specimen ID	Length, L	Length / Sweep		Length / Camber		Twist
		Top Flange	Bottom Flange	Top Flange	Bottom Flange	
	(mm)					(°)
LRC1-0.80	10977	-1800	-2484	1126	941	-0.5
LRC1-0.38	10975	1929	1266	1219	1186	0.6
LRC1-0.38 Retest	10975	2512	1424	-1220	-1220	-0.6
LRC1-0.25	10977	-1678	-2601	1568	1514	-0.2
LRC2-0.80	10981	-1788	-4575	1417	1255	-0.9
LRC2-0.38	10976	-1413	-1999	1463	998	0.7
LRC2-0.25	10975	-1742	-3976	1463	1756	0.3
LRC3-0.80	10979	-1821	-1540	1689	3658	0.6
LRC3-0.25	10979	-1212	-3277	1156	1568	0.4
LRC4-0.80	10980	2278	1388	-1464	-1938	0.9
LRC4-0.38	10978	-1861	-3347	-1098	-1220	0.9
LRC4-0.25	10975	1539	1541	1291	1186	0.7
LRC5-0.80	10984	-2554	-2255	1998	2031	0.5
LRC5-0.25	10975	3247	4480	-878	-1116	0.3

4. Experimental Test Results

Table 3 summarizes the peak loads applied at the cantilever tip and back span load point locations, P_{max} and P_b, respectively, the local maximum bending moment along the back span, M^L_{max}, the bending moment at the fulcrum support, M_{Fmax}, the normalized moment capacities for the back span and fulcrum, as well as the failure mode, where PH+ indicates plastic hinging, i.e., attaining the plastic moment capacity without experiencing instability, at the back span, PH– indicates plastic hinging at the fulcrum support, and LTB indicates inelastic LTB. The first test specimen, which was intended to be subjected to a ratio of 0.80 of the load on the back span to the load on the cantilever (κ_1''' value of 0.80), actually ended up having a 0.75 load ratio due to nuances in achieving the anticipated loading scheme in the laboratory. It should also be noted that, although the original test specimen matrix was composed of 14 specimens, LRC1-0.38 had to be retested due to an inconsistency in the load applied in the first test, which provided additional restraint to the tip of the cantilever. The results of the retest are reported as LRC1-0.38 Retest in Table 3.

Considering only the load case of 0.25, which was tested in all five LRCs, and comparing the M_{Fmax}/M_p ratios, the following observations can be drawn from the test results:

- LRC1-0.25 and LRC4-0.25 had identical M_{Fmax}/M_p ratios of 0.90. This indicates that the additional lateral brace on the bottom flange of the back span (at the load point closest to the fulcrum support) did not have noticeable effect on the moment capacity of the girder when the cantilever remained unbraced.
- LRC2-0.25 had an M_{Fmax}/M_p value of 0.95, corresponding to a 6% increase in the moment capacity compared to LRC1-0.25, suggesting that the addition of a brace at the top flange of the cantilever is more effective at increasing the moment capacity of the girder compared to providing a bottom flange brace to the back span location closest to the fulcrum.
- LRC3-0.25 provided an appreciable increase of 22% in the moment capacity compared to LRC1-0.25, and a 16% increase in moment capacity compared to LRC2-0.25, confirming that

the addition of a bottom flange brace on the cantilever tip is particularly effective at increasing the moment capacity of the overhanging girder. Similar increases in moment capacity can be seen for LRC5-0.25, since both LRC5-0.25 and LRC3-0.25 reach the full cross-sectional capacity.

- Changing the load ratio while the load on the cantilever exceeds the load on the back span has a very small impact on moment capacity, increasing the M_{Fmax}/M_p ratio by only 1% for LRC4-0.25 compared to LRC4-0.38 and by 2% when comparing LRC2-0.25 to LRC2-0.38. LRC1-0.38 Retest saw a 3% increase compared to LRC1-0.25.

Table 3: Flexural capacities and failure modes of test specimens.

Specimen ID	Maximum Load at Cantilever, P_{max} (kN)	Maximum Load at Back Span, P_b (kN)	Local Maximum Moment on Back Span, M^L_{max} (kN·m)	Maximum Moment at Fulcrum, M_{Fmax} (kN·m)	M^L_{max}/M_p	M_{Fmax}/M_p	Failure Mode
LRC1-0.80	172	138	644	334	1.01	0.52	PH+
LRC1-0.38	332	126	479	619	0.78	1.01	PH–
LRC1-0.38 Retest	315	120	473	574	0.77	0.93	LTB
LRC1-0.25	300	75	218	544	0.36	0.90	LTB
LRC2-0.75	188	141	635	409	1.01	0.65	PH+
LRC2-0.38	319	121	473	592	0.74	0.93	LTB
LRC2-0.25	330	83	211	608	0.33	0.95	LTB
LRC3-0.80	172	138	636	331	1.01	0.53	PH+
LRC3-0.25	372	93	263	686	0.42	1.10	PH–
LRC4-0.80	167	137	624	333	1.02	0.54	PH+
LRC4-0.38	301	114	409	552	0.66	0.89	LTB
LRC4-0.25	303	76	209	554	0.34	0.90	LTB
LRC5-0.80	172	138	641	332	1.00	0.52	PH+
LRC5-0.25	371	93	280	693	0.44	1.09	PH–

Nethercot (1974) proposed that the classification of lateral–torsional buckling (LTB) as inelastic depends on whether the stress at the compression flange tips reaches the yield stress of the member before buckling occurs, considering any residual stresses existing at the flange tips. Nethercot's definition of inelastic buckling is used to describe the range of buckling experienced by each of the test girders. This is determined by examining the strains recorded at the top (compression) flange of the back span for girders tested under a load ratio of 0.80, and at the bottom (compression) flange at the fulcrum support for girders tested under load ratios of 0.38 or 0.25. This analysis involves using longitudinal strain gauges and combining them with the measured residual stresses for the section. While residual stress (σ) measurement was conducted for only one heat of steel as shown in Fig. 8, the same distribution is assumed for all 14 girders for the purposes of this analysis.

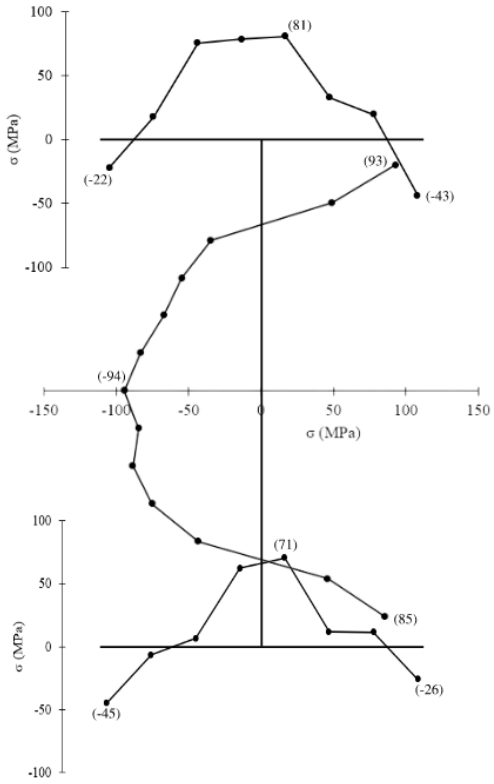

Figure 8: Residual stress distribution for the test specimen (W410×85)

The placement of four strain gauges on the bottom (compression) flange at the fulcrum support along with the cardinal directions in the laboratory (see Fig. 5b) is shown in Fig. 9a, referred to as Fulcrum Northwest, Northeast, Southwest and Southeast. Fig. 9b shows the placement of two strain gauges on the top (compression) flange on the back span, referred to as Back Span West and Back Span East, placed 100 mm north of the centreline of the second load point from the south support.

The axial stress at buckling in the longitudinal direction of the specimen, obtained from the strain gauges at the compression flange tips at the two measurement locations and normalized by the measured flange yield stress of each of the girders, $F_{y,f}$, is shown in Table 4. Positive stress ratios indicate tension and negative stress ratios indicates compression. An asterisk (*) indicates that the Fulcrum Southeast strain gauge reading is presented due to the Fulcrum Northeast strain gauge malfunctioning during the test.

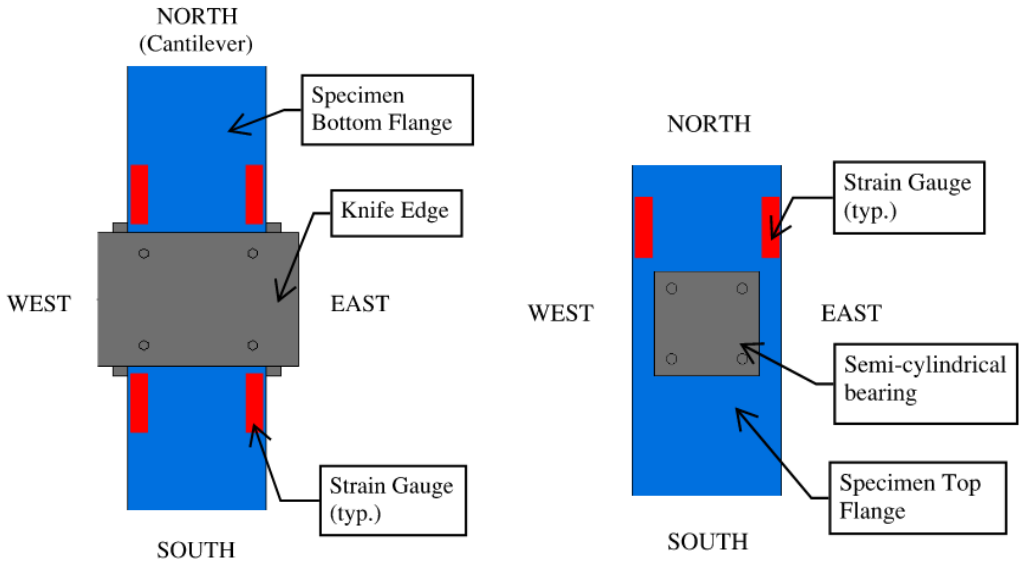

a) Strain gauges at fulcrum b) Strain gauges at back span

Figure 9: Strain gauge locations (see Fig. 5b for cardinal directions in the laboratory)

Table 4: Longitudinal stresses of compression flange at buckling

Specimen ID	Axial Stress Ratio			
	Back Span East	Back Span West	Fulcrum Northeast	Fulcrum Northwest
LRC1-0.80	-1.0	-1.0	-0.6	-0.6
LRC1-0.38	-0.8	-0.7	-1.0	-1.0
LRC1-0.38 Retest	-0.7	-0.7	-0.8	-1.0
LRC1-0.25	-0.4	-0.4	-0.9	-1.0
LRC2-0.75	-1.0	-1.0	-0.8	-0.5
LRC2-0.38	-0.8	-0.6	-0.8	-1.0
LRC2-0.25	-0.4	-0.3	-1.0*	-1.0
LRC3-0.80	-1.0	-1.0	-0.7	-0.7
LRC3-0.25	-0.4	-0.4	-1.0*	-1.0
LRC4-0.80	-1.0	-1.0	-0.4	-0.7
LRC4-0.38	-0.6	–	-0.9	-1.0
LRC4-0.25	-0.4	-0.3	-0.9	-1.0
LRC5-0.80	-1.0	–	-0.6	-0.6
LRC5-0.25	-0.4	-0.6	-1.0*	-1.0

According to strain gauge readings alone, all girders experienced flexural yielding at buckling at the compression flange tips, as shown in Table 4. Since the residual stress results showed compressive residual stresses at the flange tips, the net stress present at the compression flange tips at buckling exceeds the compressive stress obtained from the longitudinal strain gauges, and all girders with M_{max}/M_p less than 1.00 are classified as having buckled in the inelastic range.

5. Implication of Test Results in Design of Gerber System

The Canadian Institute of Steel Construction (CISC) Design Module 8 on Single-Storey Building Design (Lasby 2019) outlines a design procedure for overhanging girders which requires treating the cantilever and back span segments separately, calculating a moment resistance for each segment. The cantilever is checked under negative bending moment using the Essa and Kennedy (1993) interaction method, which assumes the entire length of the back span is unbraced. Essa and

Kennedy (1993) provide interaction factors for the cases of an unbraced cantilever tip or top flange restraint at the tip; for cases of both top and bottom flange bracing at the cantilever tip, the moment resistance of the cantilever segment is calculated using Schmitke and Kennedy (1985)'s effective length factors, as suggested by Essa and Kennedy (1994).

Nominal moment resistances according to the CISC method were calculated for each of the test girders in the study, and the results along with test-to-predicted ratios and percent errors are presented in Table 5. For ease of comparison, the negative moment at the fulcrum corresponding to the resistance of the back span under positive moment is calculated, and the nominal resistance reported from the CISC method is taken as the minimum of the three nominal moment resistances at the fulcrum, which is then compared against the maximum experimental fulcrum moment, M_{Fmax}. The CISC moment resistance which governed is also shown, where 'C' indicates the minimum CISC moment resistance was that of the cantilever, 'B(–)' indicates back span under negative bending moment, and 'B(+)' indicates back span under positive bending moment. In the case of two symbols given for a single specimen, these checks give capacities within 1% of each other.

Table 5: Comparison of experimental moment resistances with CISC method (2019) predictions

Specimen ID	Maximum Experimental Moment, M_{Fmax} (kN·m)	CISC (2019) Moment Resistance (kN·m)	Governing CISC Resistance	Test/Predicted	% Error
LRC1-0.80	334	254	C, B(–)	1.31	24.0
LRC1-0.38	619	246	C	2.52	60.3
LRC1-0.38 Retest	574	252	C	2.28	56.1
LRC1-0.25	544	250	B(–)	2.18	54.0
LRC2-0.75	409	244	B(–)	1.68	40.3
LRC2-0.38	592	249	B(+)	2.38	57.9
LRC2-0.25	608	251	C, B(–)	2.42	58.7
LRC3-0.80	331	245	B(+)	1.35	26.0
LRC3-0.25	686	458	C	1.50	33.2
LRC4-0.80	333	307	C	1.08	7.8
LRC4-0.38	552	434	B(–)	1.27	21.4
LRC4-0.25	554	428	C	1.29	22.7
LRC5-0.80	332	321	C	1.03	3.3
LRC5-0.25	693	635	C	1.09	8.4

In Table 5, a test-to-predicted ratio greater than 1.0, and a positive percent error, indicates that the CISC design method is conservative. Referring to this table, the CISC approach (2019) provides conservative predictions of moment capacity for all test girders, especially underestimating the capacity of girders tested under load ratios of 0.38 and 0.25 which failed by inelastic LTB. This is largely due to two conservative assumptions made in the design method which do not reflect the circumstances seen in the tests. The first of these assumptions concerns the bracing provided to the back span. While all test girders had lateral bracing provided to the top flange of the back span at 1.83 m intervals, the CISC method for predicting the capacity of the back span under negative bending moments assumes the entire length of the back span is unbraced. Since the majority of the top flange of the back span in the test girders is under compression, this assumption by the CISC method is therefore conservative. The second conservative assumption made when following the

CISC design procedure is that the girder is free to warp at the fulcrum when checking the cantilever segment and free to warp at both supports when analyzing the back span. However, the test girders were subjected to a certain degree of warping restraint at the supports stemming from the test setup fixtures as well as the flexural stiffness of the adjacent span of the overhanging girder. This additional restraint would lead to higher capacities than what would be obtained if the girder was completely free to warp at the supports, particularly at the fulcrum.

6. Conclusions

A full-scale physical testing program was developed to investigate the effect of various influential parameters, such as loading and bracing conditions, on the stability response of Gerber systems. The experimental study consisted of 14 W410×85 (Class 1) single-overhanging girders, with back span and cantilever lengths of 9.14 m and 1.83 m, respectively. The design of the test setup was based largely on preliminary FE simulations of the test specimens which provided the anticipated loads and displacements in the tests. Initial geometric imperfections and material properties were measured for all test specimens prior to testing.

The experimental results, including the obtained moment capacity and stress data, were presented for the test specimen. The flexural capacities were finally used to evaluate the CISC design method for Gerber system. The key findings of this study are summarized as follows:

- When the cantilever tip is left unbraced, introducing a lateral brace to the bottom flange at the back span load location nearest to the fulcrum support has negligible impact on the moment resistance of the girder.
- Implementing bracing on the top flange of the cantilever tip proves more effective in enhancing the moment capacity of a single-overhanging girder by 6% when contrasted with adding a bottom flange brace on the back span while keeping the cantilever unbraced.
- The addition of a bottom flange lateral brace at the cantilever tip increased the moment capacity of the girder by 16% compared to when the bottom flange remained unbraced.
- The moment resistances predicted by CISC Design Module 8 (Lasby 2019) are generally conservative compared to the tested overhanging girders' flexural capacities, primarily due to conservative assumptions associated with this method surrounding lateral bracing on the back span and warping restraint at the supports.

Future studies are needed to further evaluate the available design procedures for overhanging beams and propose a test-based design method that can be used to estimate the flexural capacity of overhanging beams with the loading and bracing conditions prevailing in Gerber construction in North America.

Acknowledgments

Financial support for this research was provided by the Natural Sciences and Engineering Research Council of Canada and Canadian Institute of Steel Construction (CISC). The authors would like to acknowledge the financial support by the CISC Centre for Steel Structures Education and Research (the Steel Centre) at the University of Alberta. Financial support in the form of scholarships from the University of Alberta, DIALOG, and the Canadian Institute of Steel Construction is gratefully acknowledged. All steel materials for the test specimens and ancillary testing fixtures were donated by Supreme Group. Finally, the authors would like to thank Mr.

Vahab Esmaeili, Ph.D. student at the University of Alberta, for providing numerical simulation results and offering input in designing the test program.

References

AISC. (2022). *ANSI/AISC 360-22 Specification for Structural Steel Buildings*. American Institute of Steel Construction, Chicago, IL.

CISC. (1989). "Roof Framing with Cantilever (Gerber) Girders & Open Web Steel Joists." Canadian Institute of Steel Construction, Willowdale.

Closkey, Dan J. (1988). "Report of the Commissioner Inquiry Station Square Development." Province of British Columbia, Burnaby, BC.

CSA. (2019). *CSA S16-19 Design of Steel Structures*. Canadian Standards Association, Toronto, ON.

Driver, R. G., Kulak, G. L., Elwi, A. E., and Kennedy, D. J. L. (1997). "Seismic behaviour of steel plate shear walls." Structural Engineering Report No. 215, University of Alberta, Edmonton, AB.

Esmaeili, V., Imanpour, A., and Driver, R. G. (2021). "Stability of Gerber Systems with Top-flange Bracing." *Annual Stability Conference*, Structural Stability Research Council, Louisville, KY.

Essa, H. S., and Kennedy, D. J. L. (1994). "Design of Cantilever Steel Beams: Refined Approach." *Journal of Structural Engineering*, 120, 2623–2636.

Essa, H. S., and Kennedy, D. J. L. (1993). "Distortional Buckling of Steel Beams." Structural Engineering Report No. 185, University of Alberta, Edmonton, AB.

Galambos, T. V. (1988). *Guide to stability design criteria for metal structures*. 4th Ed., John Wiley & Sons, Inc., New York.

Kirby, P. A., and Nethercot, D. A. (1979). *Design for Structural Stability.* John Wiley & Sons, Inc., New York.

Lasby, R. M. (2019). "CISC Design Module 8 – Single-Storey Building Design." Canadian Institute of Steel Construction, Markham, Ontario.

Metten, A. (2019). "Structural Design of the Gerber Girder Cantilever System – Filling the Knowledge Gap [Conference presentation]." *The Canadian Steel Conference*, Canadian Institute of Steel Construction, Montreal, Quebec.

Nethercot, D. A. (1974). "Residual stresses and their influence upon the lateral buckling of rolled steel beams." *The Structural Engineer*, 52(3), 89–96.

Nethercot, D. A. (1973). "The Effective Lengths of Cantilevers as Governed by Lateral Buckling." *The Structural Engineer*, 51(5), 161–168.

Roeder, C. W., and Assadi, M. (1982). "Lateral Stability of I-beams with Partial Supports." *Journal of the Structural Division*, 108(8), 1768–1780.

Rongoe, J. (1996). "Design Guideline for Continuous Beams Supporting Steel Joist Roof Structures." *NASCC Proceedings.*

Timoshenko, S. P., and Gere, J. M. (1961). *Theory of Elastic Stability*. McGraw-Hill, New York.

Trahair, N. S. (1983). "Lateral Buckling of Overhanging Beams." *International Conference on Instability and Plastic Collapse of Steel Structures*, Manchester, Granada Publishing, London.

Yarimci, E., Yura, J. A., and Lu, L-W. (1967). "Techniques for testing structures permitted to sway." *Experimental Mechanics*, 7(8), 321–331.

Yura, J. A., and Helwig, T. A. (2010). "Buckling of Beams with Inflection Points." *Proceedings of the Annual Stability Council*, Structural Stability Research Council, Florida.

Ziemian, R. D. (2010). *Guide to Stability Design Criteria for Metal Structures*. 6th Ed., John Wiley & Sons, Inc., Hoboken, NJ.